

Robust Iterative Learning Control of Single-phase Grid-connected Inverter

Zhong-Qiang Wu Chun-Hua Xu Yang Yang

Key Lab of Industrial Computer Control Engineering of Hebei Province, Yanshan University, Qinhuangdao 066004, China

Abstract: For the single phase inductance-capacitance-inductance (LCL) grid-connected inverter in micro-grid, a kind of robust iterative learning controller is designed. Based on the output power droop characteristics of inverter, the current sharing among the inverters is achieved. Iterative learning strategy is suitable for repeated tracking control and inhibiting periodic disturbance, and is designed using robust performance index, so that it has the ability to overcome the uncertainty of system parameters. Compared with the repetitive control, the robust iterative learning control can get high precision output waveform, and enhance the tracking ability for waveform, and the distortion problem of the output signal can be solved effectively.

Keywords: Inductance-capacitance-inductance (LCL) filter, iterative learning, robust control, power droop-characteristics, repetitive control.

1 Introduction

Micro-grid as an autonomous system, which can realize self-protection, self-management and self-control, can either run in parallel with the utility grid, or run alone. Based on the characteristics of flexibility, stability and easy management, micro-grid is being paid more and more attention^[1]. The power sources of micro-grid consist of many micro-sources, such as micro-gas turbine, fuel cell, photovoltaic battery, super capacitor, flywheel energy storage device, and battery, etc. The micro-sources are on the user side, which supply the electricity and heat energy for users, and have the characteristics of low cost, low voltage, low pollution, etc^[2].

The grid-connected inverter is the interface device of energy conversion in micro-grid; and its performance is important in the stability and efficient operation of system^[3]. In the micro-grid, wind generator, fuel cell and solar cell supply distributed power and cascade the utility grid through the grid-connected inverter. All the parallel inverters must run synchronously to guarantee the flexibility and reliability of micro-grid, and the electric and thermal stress of modules are to be distributed uniformly and reasonably^[4]. In the micro-grid, the parallel control schemes of inverters are generally divided into centralized control, master-slave control, disperse logic control and no interconnection line control, etc^[5]. In the first three schemes, there are many interconnection lines among the inverters, which leads to the complexity of signal transmission, and reduce the reliability of system. The fourth scheme can eliminate the problem that the parallel system cannot work normally, which is caused by signal interference among the micro-grid interconnection lines in the distribution control^[6].

On one hand, for the single-phase grid-connected inverter, inductance-capacitance-inductance (LCL) filter can suppress high-frequency harmonics effectively. On the other

hand, it is easy to cause the oscillation of system output. LCL inverters generally adopt two control strategies: One is called the indirect current control which is based on inductive current feedback on inverter side. The other is called the direct current control which is based on inductive current feedback on power network side. The former may cause phase error, which is difficult to make the net current satisfy unity power factor, and is difficult to be controlled when the system parameters are changed, while the latter scheme solves these problems very well.

For the single-phase LCL grid-connected inverter in micro-grid, we adopt no interconnection line control based on power droop characteristic, which realizes the current sharing among the inverters. In proportional-integral-derivative (PID) control, it has the defect that it cannot track periodical signal accurately and is difficult to set controller parameters^[7-9]. In this paper, a kind of robust iterative learning controller is adopted based on direct current feedback, which improves the robustness of system by robust performance index, and it also improves the ability of system tracking periodic and repetitive signal by the iterative learning.

2 The no interconnection line control based on power droop characteristic

In the control without interconnection line, there is no other signal interconnection line among modules except the load line, which can improve the reliability of system. The principal figure of parallel inverter without interconnection line in micro-grid is shown in Fig. 1, in which power generation system includes solar power inverters and the load on the AC bus.

For convenience, we only consider two inverter sources supplying power for the same load, the equivalent circuit is shown in Fig. 2.

In Fig. 2, E is the voltage of load, the output impedances of inverters 1 and 2 can be written as

$$R_i + jX_i = Z_i \angle \theta_{z_i}, \quad i = 1, 2. \quad (1)$$

Regular paper
Manuscript received April 12, 2013; revised September 12, 2013
This work was supported by Natural Science Foundation of Hebei Province (No. F2012203088).

In (1), $Z_i = \sqrt{R_i^2 + X_i^2}$, θ_1, θ_2 are two phases of inverter output voltage; θ_{z_1} and θ_{z_2} are the phases of equivalent output impedance. The output power of solar power inverter can be described as

$$P_i = \frac{E_i E \cos(\theta_{z_i} - \theta_i) - E_i \cos \theta_{z_i}}{Z_i} \quad (2)$$

$$Q_i = \frac{E_i E \sin(\theta_{z_i} - \theta_i) - E_i \sin \theta_{z_i}}{Z_i}. \quad (3)$$

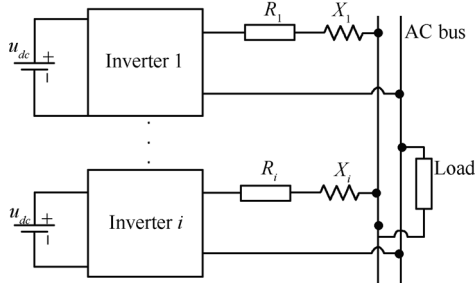


Fig. 1 Parallel inverter without interconnection line in Micro-grid

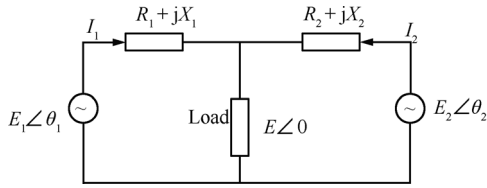


Fig. 2 The parallel equivalent circuit of inverters

Assume that the equivalent output impedance is inductive, and $\sin \theta_i \approx \theta_i$. Because there is only small phase error between the inverter output voltage and the system voltage, it can be concluded that the active power of the inverter output power mainly depends on θ_1 , reactive power mainly depends on amplitude E_i according to (2) and (3)^[10].

Based on the above analysis, the frequency and amplitude of the inverter output voltage can be controlled based on the power droop characteristic in (4) and (5), which can share load current and inhibit circulating current:

$$\omega_i = \omega_0 - \frac{\Delta \omega_{\max}}{P_{ei}} P_i = \omega_0 - m_i P_i \quad (4)$$

$$E_i = E_0 - \frac{\Delta E_{\max}}{Q_{ei}} Q_i = E_0 - n_i Q_i \quad (5)$$

where ω_0 and E_0 are the angular frequency and amplitude of output voltage, respectively; $\Delta \omega_{\max}$ and ΔE_{\max} are the maximum changes in value of system frequency and system voltage amplitude, respectively; P_{ei} and Q_{ei} are the rated active power and reactive power of inverter, respectively; m_i and n_i are the droop coefficients of the frequency and amplitude, respectively.

By (4) and (5), it is known that changing the frequency of inverter output voltage can control the active power; and changing the amplitude of inverter output voltage can control the reactive power. While inverter is running in parallel, each power module is regulated according to ω_i and E_i by P_i and Q_i , which realizes the load current sharing,

and guarantees the uniform distribution of electric stress among the modules, and realizes current balance of each module. When the input voltage and load current change, each module can ensure the stability of output voltage, and has good transient characteristics in current sharing at the same time^[11].

3 The model of single-phase LCL voltage source inverter

The structure of single-phase LCL voltage source grid-connection inverter is shown in Fig. 3.

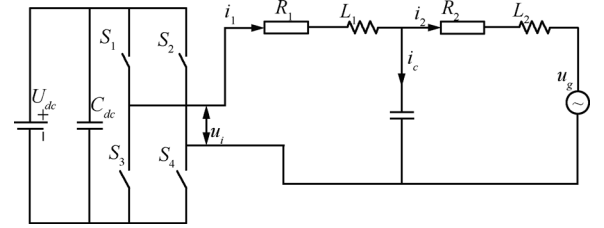


Fig. 3 The structure of single-phase LCL voltage source grid-connection inverter

In Fig. 3, U_{dc} and u are DC output voltages of electrical power generating system and the output voltage of grid-connection inverter, respectively. C_{dc} is filter capacitor on DC side; $S_1 - S_4$ represent 4 IGBT switch tubes in inverter bridge; L_1 and R_1 are inductance and parasitic resistance on inverter side, respectively; L_2 and R_2 are inductance and parasitic resistance on grid side, respectively; C is filter capacitor on the AC side, u_g is the voltage of local user.

According to the Kirchhoff's law, we can get

$$\begin{cases} \dot{i}_1 = -\frac{R_1}{L_1} i_1 - \frac{u_c}{L_1} + \frac{u}{L_1}, \\ \dot{u}_c = \frac{1}{C} (i_1 - i_2), \\ \dot{i}_2 = -\frac{R_2}{L_2} i_2 + \frac{u_c}{L_2} - \frac{u_g}{L_2}. \end{cases} \quad (6)$$

The transfer function from the output voltage of the inverter bridge u to the grid side inductance current i_2 is

$$G(s) = \frac{1}{a_1 s^3 + a_2 s^2 + a_3 s + a_4} \quad (7)$$

where $a_1 = CL_1 L_2$, $a_2 = (R_1 R_2 C + L_1 + L_2)$, $a_3 = (CL_1 R_2 + CL_2 R_1)$, $a_4 = R_1 + R_2$.

The open loop transfer function of system is given by

$$y(s) = G(s)u(s) \quad (8)$$

where $y(s)$ is the Laplace transform of output current i_2 :

$$\dot{x} = A_G x + B_G u + B_w u_g \quad (9)$$

$$y = C_G x. \quad (10)$$

In (9) and (10), $x = [i_1 \quad u_c \quad i_2]^T$, $A_G = \begin{bmatrix} -\frac{R_1}{L_1} & -\frac{1}{L_1} & 0 \\ \frac{1}{C} & 0 & -\frac{1}{C} \\ 0 & \frac{1}{L_2} & -\frac{R_2}{L_2} \end{bmatrix}$, $B_G = [\frac{1}{L_1} \quad 0 \quad 0]^T$, $B_w = [0 \quad 0 \quad -\frac{1}{L_2}]^T$, $C_G = [0 \quad 0 \quad 1]$.

If PID control strategy is adopted for the system (7) by direct-current feedback, oscillation phenomenon is produced easily, which causes waveform distortion of output current, and cannot track periodic signal accurately^[12]. In this paper, a kind of robust iterative learning control is adopted, which can improve the tracking ability for periodic signals.

4 The existence conditions of robust iterative learning controller

Equation (8) can be rewritten as iterative learning mode as

$$y_k(s) = G(s)u_k(s) \quad (11)$$

where $y_k(s)$ is the k -th iteration of the system output, $u_k(s)$ is the k -th iterations of the system input. The k -th error of system output is

$$e_k(s) = y_d(s) - y_k(s) \quad (12)$$

where $y_d(s)$ is the expected output.

Based on iterative learning control law of the error feedback, the control law is designed by

$$u_{k+1}(s) = u_k(s) + K(s)e_{k+1}(s). \quad (13)$$

In order to guarantee system convergence in the process of iterative learning, the controller $K(s)$ which we need to design must be stable^[13].

Assume that the initial error is zero, the tracking error can be got through (10) and (11):

$$e_{k+1}(s) = (1 + G(s)K(s))^{-1}e_k(s) = F(s)e_k(s). \quad (14)$$

Putting $F(s) = (1 + G(s)K(s))^{-1}$ as error transfer function, we can get robust iterative learning control of closed-loop system by (10)–(12):

$$y_k(s) = (1 + G(s)K(s))^{-1}G(s)K(s)y_d(s) + G(s)u_{k-1}(s) \quad (15)$$

where the input $u_k(s)$ can be obtained by the $(k-1)$ -th error iteration; and its initial error is zero, which can be ignored by analyzing the stability of (15)^[13]. For the stability of system (14), we only need to discuss the stability of $(1 + G(s)K(s))^{-1}G(s)K(s)$. The existing condition of robust iterative learning controller is given by Theorem 1.

Theorem 1. Assume $G(s)$ and $K(s)$ are stable, for a closed loop control system, $y(s) = \frac{G(s)}{1+G(s)K(s)}u(s)$, the sufficient condition of closed loop system stability is $\|G(s)K(s)\|_\infty < 1$.

Proof. The state space realization of $G(s)$ and $K(s)$ are

$$G(s)K(s) = \{A, B, C, D\} \quad (16)$$

where $A = \begin{bmatrix} A_G & B_G C_K \\ 0 & A_K \end{bmatrix}$, $B = \begin{bmatrix} B_G D_K \\ B_K \end{bmatrix}$, $C = \begin{bmatrix} C_G & D_G C_K \end{bmatrix}$, $D = D_G D_K$, $G(s) = \{A_G, B_G, C_G, D_G\}$, $K(s) = \{A_K, B_K, C_K, D_K\}$.

As $\|G(s)K(s)\|_\infty < 1$, the equivalent Riccati equation is

$$\begin{aligned} & (A + BR^{-1}D^T C)^T X + X (A + BR^{-1}D^T C) + \\ & XBR^{-1}B^T X + C^T S^{-1}C = 0. \end{aligned} \quad (17)$$

where $R = I - D^T D$, $S = I - DD^T$. Equation (17) has semi positive definite solution $X \geq 0$ and $A + BR^{-1}D^T C + BR^{-1}B^T X$ is stable.

In order to get the conclusion, we just need to prove that the matrix \bar{A} in the following equation is stable:

$$\bar{A} = A - B(I + D)^{-1}C. \quad (18)$$

The Riccati equation (16) can be written as

$$\begin{aligned} & \bar{A}^T X + X \bar{A} + \left[XB + C^T (I + D^T)^{-1} (I + D) \right] R^{-1} \\ & \left[B^T X + (I + D^T) (I + D)^{-1} C \right] = 0. \end{aligned} \quad (19)$$

If \bar{A} is not stable, $\text{Re } \lambda \geq 0$ for the characteristic value λ of \bar{A} . Set the corresponding feature vector ε as

$$\bar{A}\varepsilon = \lambda\varepsilon. \quad (20)$$

Multiply (19) on left by ε and on right by the adjoint matrix $n\varepsilon^*$:

$$\varepsilon^* X \varepsilon (\lambda + \bar{\lambda}) + \eta^* R^{-1} \eta = 0 \quad (21)$$

$$\eta = \left[B^T X + (I + D^T) (I + D)^{-1} C \right] \varepsilon \quad (22)$$

where $\bar{\lambda}$ is the conjugate value of λ . $\text{Re } \lambda \geq 0$, $X \geq 0$, $R > 0$, so $\eta = 0$.

$$B^T X \varepsilon = - \left(I + D^T \right) (I + D)^{-1} C \varepsilon. \quad (23)$$

According to (23), we have

$$\bar{A}\varepsilon = \left(A + BR^{-1}D^T C + BR^{-1}B^T X \right) \varepsilon = \lambda\varepsilon. \quad (24)$$

The stability of (24) and the stability of $A + BR^{-1}D^T C + BR^{-1}B^T X$ are contradictory, so \bar{A} is stable, which proves Theorem 1. \square

5 The design of robust iterative learning controller

According to Theorem 1, it is known that the sufficient condition to stabilized closed-loop system (15) is $\|G(s)K(s)\|_\infty < 1$. As shown in Fig. 4, we deduce the specific method of getting $K(s)$ by introducing the multiplicative uncertain systems. The actual system $G_A(s)$ belongs to unstructured set^[14].

$$U_A = \{G_A(s) = [I + W(s)\Delta(s)]G(s), \Delta(s) \in \overline{BH}_\infty\}. \quad (25)$$

where $W(s)$ is the weight function, \overline{BH}_∞ is the robust performance index. The problem which makes U_A robust stable is looking for a feedback controller $K(s)$, so that the closed loop control system is stable for any $\Delta(s) \in \overline{BH}_\infty$.

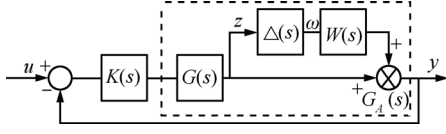


Fig. 4 The closed loop control system with multiplicative uncertainty

The transfer function from ω to z is

$$z = -(I + K(s)G(s))^{-1}G(s)K(s)W(s). \quad (26)$$

For the unstructured set U_A , there is stable controller $K(s)$, when $\Delta(s)=0$. The closed loop control system is stable when (26) is got.

The sensitivity function of output side is

$$T(s) = [I + G(s)K(s)]^{-1}G(s)K(s). \quad (27)$$

Equation (26) can be rewritten as

$$\|T(s)W(s)\|_{\infty} < 1. \quad (28)$$

For robust stabilization of system (15), the sufficient condition can be translated into the weighted constraint conditions of sensitivity function matrix. Thus, the robust stabilization problem of closed-loop system (15) can be transformed into H_{∞} control problem^[15].

Let

$$M(s) = \begin{bmatrix} 0 & W(s) \\ I & -G(s) \end{bmatrix}. \quad (29)$$

Firstly, $M(s)$ is decomposed, and the state space model is got as

$$M(s) = \begin{bmatrix} M_{11}(s) & M_{12}(s) \\ M_{21}(s) & M_{22}(s) \end{bmatrix} = \begin{bmatrix} A & B_1 & B_2 \\ C_1 & D_{11} & D_{12} \\ C_2 & D_{21} & D_{22} \end{bmatrix}$$

where $M_{ij}(s) = C_i(s)(sI - A)^{-1}B_j + D_{ij}$.

$G(s)$ is got for single phase LCL grid-connected inverter:

$$G(s) = \begin{bmatrix} A_G & B_G \\ C_G & 0 \end{bmatrix} = C_G(sI - A_G)^{-1}B_G.$$

At the same time, the weighted function is defined as

$$W(s) = \begin{bmatrix} A_{\omega} & B_{\omega} \\ C_{\omega} & D_{\omega} \end{bmatrix} = C_{\omega}(sI - A_{\omega})^{-1}B_{\omega}$$

where $A_G \in \mathbf{R}^{n_p \times n_p}$, $B_G \in \mathbf{R}^{n_p \times m}$, $C_G \in \mathbf{R}^{p \times n_p}$, $A_{\omega} \in \mathbf{R}^{n_w \times n_w}$, $B_{\omega} \in \mathbf{R}^{n_w \times m}$, $C_{\omega} \in \mathbf{R}^{m \times n_w}$.

The state space of $M(s)$ can be got through $M_{ij}(s)$, $G(s)$, $W(s)$ and (29) as

$$M(s) = \begin{bmatrix} A & B_1 & B_2 \\ C_1 & D_{11} & D_{12} \\ C_2 & D_{21} & D_{22} \end{bmatrix} = \begin{bmatrix} A_{\omega} & 0 & 0 & B_{\omega} \\ 0 & A_G & 0 & -B_G \\ C_{\omega} & 0 & 0 & I_m \\ 0 & C_G & I_G & 0 \end{bmatrix}$$

where $A = \begin{bmatrix} A_{\omega} & 0 \\ 0 & A_G \end{bmatrix}$, $B_1 = \begin{bmatrix} 0 \\ 0 \end{bmatrix}$, $B_2 = \begin{bmatrix} B_{\omega} \\ -B_G \end{bmatrix}$, $C_1 = \begin{bmatrix} C_{\omega} & 0 \end{bmatrix}$, $C_2 = \begin{bmatrix} 0 & C_G \end{bmatrix}$, $D_{11} = 0$, $D_{12} = I_m$, $D_{21} = I_G$, $D_{22} = 0$.

For H_{∞} controller satisfying the output feedback condition and $M(s)$, define

$$R = \begin{bmatrix} D_{11}^T D_{11} - D_{21} & D_{11}^T D_{21} \\ D_{12}^T D_{11} & D_{12}^T D_{12} \end{bmatrix} \quad (30)$$

$$\tilde{R} = \begin{bmatrix} D_{11} D_{11}^T - D_{12} & D_{11} D_{21}^T \\ D_{21} D_{11}^T & D_{21} D_{21}^T \end{bmatrix}. \quad (31)$$

If R^{-1} and \tilde{R}^{-1} exist, the Hamilton matrix can be defined as

$$\bar{H}_{\infty} = \begin{bmatrix} A_H & B_H \\ C_H & D_H \end{bmatrix}$$

$$\bar{J}_{\infty} = \begin{bmatrix} A_J & B_J \\ C_J & D_J \end{bmatrix}$$

where $A_H = A - [B_1 \ B_2]R^{-1} \begin{bmatrix} D_{11}^T \\ D_{12}^T \end{bmatrix}$

$$B_H = -[B_1 \ B_2]R^{-1} \begin{bmatrix} B_1^T \\ B_2^T \end{bmatrix}$$

$$C_H = -C_1 C_1^T + C_1^T [D_{11} \ D_{12}]R^{-1} \begin{bmatrix} D_{11}^T \\ D_{12}^T \end{bmatrix} C_1$$

$$D_H = -A^T + [D_{11} \ D_{12}]R^{-1} \begin{bmatrix} B_1^T \\ B_2^T \end{bmatrix}$$

$$A_J = A^T - [C_1^T \ C_2^T]\tilde{R}^{-1} \begin{bmatrix} D_{11} \\ D_{12} \end{bmatrix} B_1^T$$

$$B_J = -[C_1^T \ C_2^T]\tilde{R}^{-1} \begin{bmatrix} C_1 \\ C_2 \end{bmatrix}$$

$$C_J = -B_1 B_1^T + B_1 [D_{11}^T \ D_{12}^T]\tilde{R}^{-1} \begin{bmatrix} D_{11} \\ D_{12} \end{bmatrix} B_1^T$$

$$D_J = -A + B_1 [D_{11}^T \ D_{12}^T]\tilde{R}^{-1} \begin{bmatrix} C_1 \\ C_2 \end{bmatrix}.$$

Through \bar{H}_{∞} , \bar{J}_{∞} and $M(s)$, we can get

$$H_x = \begin{bmatrix} A_x & B_x \\ C_x & D_x \end{bmatrix}$$

$$J_y = \begin{bmatrix} A_y & B_y \\ C_y & D_y \end{bmatrix}$$

where

$$A_x = \begin{bmatrix} A_{\omega} - B_{\omega} C_{\omega} & 0 \\ B_G C_{\omega} & A_G \end{bmatrix}$$

$$B_x = \begin{bmatrix} -B_{\omega} B_{\omega}^T & B_{\omega} B_G^T \\ B_G B_{\omega}^T & -B_G B_G^T \end{bmatrix}$$

$$C_x = C_y = \begin{bmatrix} 0 & 0 \\ 0 & 0 \end{bmatrix}$$

$$\begin{aligned}
 D_x &= \begin{bmatrix} -(A_w - B_w C_w)^T & -C_w^T B_G^T \\ 0 & -A_G^T \end{bmatrix} \\
 A_y &= \begin{bmatrix} A_w^T & 0 \\ 0 & A_G^T \end{bmatrix} \\
 B_y &= \begin{bmatrix} -C_w^T C_w & 0 \\ 0 & C_G^T C_G \end{bmatrix} \\
 D_y &= \begin{bmatrix} -A_w & 0 \\ 0 & -A_G \end{bmatrix}.
 \end{aligned}$$

The stable eigenvalue of Hamilton matrix H_x, J_x is the solution of Riccati equations. In other words, if the three conditions $X = Ric(H_x) \geq 0, Y = Ric(J_y) \geq 0$ and $I - YX \geq 0$ are satisfied, the controller $K(s)$ exists, which make the closed-loop control system (15) stable. The robust stable controller is^[15]

$$K(s) = \begin{bmatrix} A_{xy} & -L_{xy} \\ F_{xy} & 0 \end{bmatrix} \quad (32)$$

where

$$A_{xy} = \begin{bmatrix} A_w & 0 \\ 0 & A_G \end{bmatrix} + L_{xy} \begin{bmatrix} 0 & C_G \end{bmatrix} + \begin{bmatrix} B_w \\ -B_G \end{bmatrix} F_{xy}$$

$$L_{xy} = -(I - YX)^{-1} Y \begin{bmatrix} 0 \\ C_p^T \end{bmatrix}$$

$$F_{xy} = - \left[X \begin{bmatrix} B_w \\ -B_G \end{bmatrix} + \begin{bmatrix} C_w^T \\ 0 \end{bmatrix} \right]^T.$$

For all kinds of learning system, iterative learning speed is an important concept, learning speed is to study which factors related to the system output converge into a given

performance index under various learning laws. In iterative learning control, taking some effective measures can accelerate the convergence speed. It has been shown that the higher-order learning law can improve the convergence rate. Jay H. Lee pointed out that comparing with λ norm, the supremum norm can greatly improve the dynamic process of learning, so the optimal norm or H_∞ norm can be chosen. In this paper, H_∞ norm is chosen so that the optimal learning rate can be obtained.

6 Simulation research

The simulation is considered for two inverters without interconnecting line in Micro-grid, and the simulation principal diagram of each inverter is shown in Fig. 5

The parameters of each inverter are as follows: Inverter capacity is 2kVA, switch frequency is 20kHz, output voltage without load is 220V, $L_1=4$ mH, $U_{dc}=400$ V, $L_2=1$ mH, $R_1=R_2 = 0.1 \Omega, C = 10 \mu F$.

First, we compare the robust iterative learning control with the repetitive control for the tracking ability to periodic signal. The parameters of controller are determined according to [16, 17]: The simulation curve is shown in Fig. 6.

The error current curve adopting repetitive control is as shown in Fig. 7.

When adopting robust iterative learning control, the weighted function is elected as $w(s) = \frac{50}{s+50}$. From (33), we can get

$$K(s) = \frac{-37.05s^3 - 2.83 \times 10^7 s^2 - 1.01 \times 10^{10} s - 4.36 \times 10^{11}}{s^4 + 1.72 \times 10^4 s^3 + 3.83 \times 10^9 s^2 + 3.02 \times 10^{12} s + 1.41 \times 10^{14}}$$

The simulation curve is shown in Fig. 8.

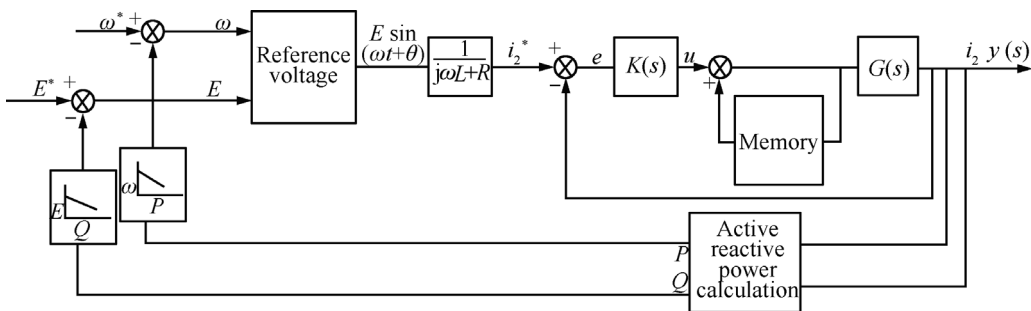


Fig. 5 The simulation principle diagram

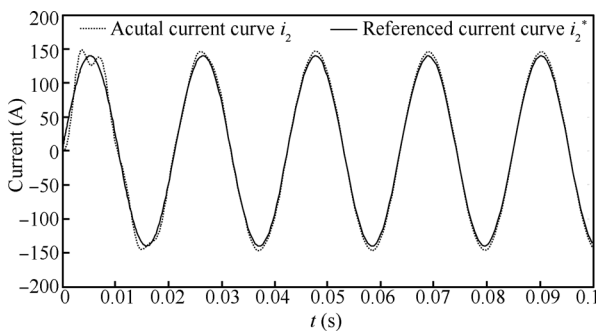


Fig. 6 The current curve adopting repetitive control

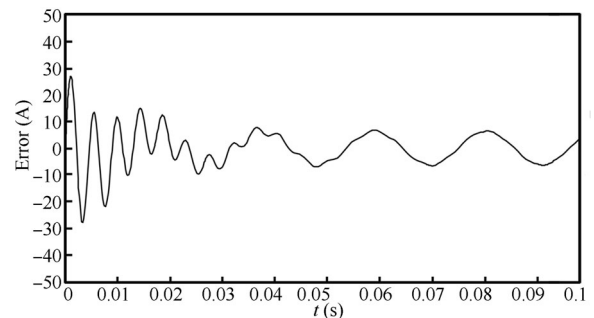


Fig. 7 The error current curve adopting repetitive control

The error current curve adopting robust iterative learning control is as shown in Fig. 9.

From Figs. 6–9, it is shown that the robust iterative learning control begins to converge through 5th iteration, and the error precision of the repetitive control is less than 10^{-1} , and the error precision of robust iterative learning control is less than 10^{-4} . The latter improves the accuracy of the output waveform, and realizes the accurate track of amplitude, phase, and frequency between system output and expected output.

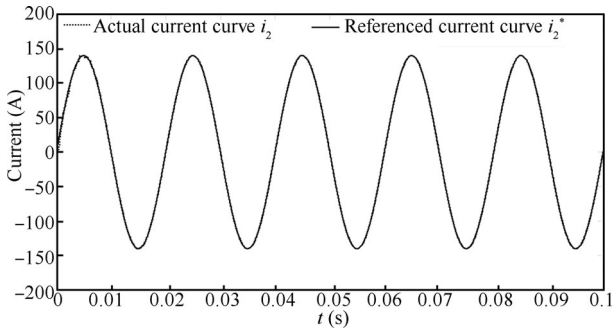


Fig. 8 The actual and reference current curve adopting robust iterative learning control

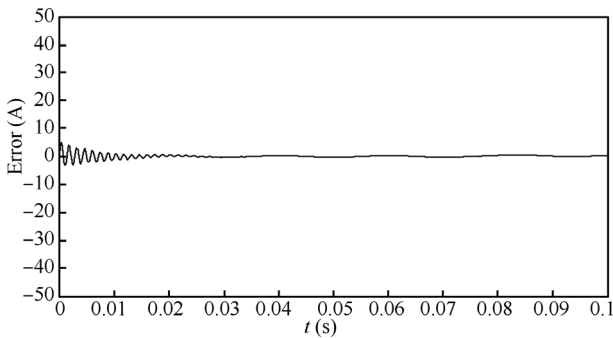


Fig. 9 The current error curve adopting robust iterative learning control

In order to test the robustness of the scheme, the parameters of system are changed as: $L_1 = 2.5 \text{ mH}$, $L_2 = 1.5 \text{ mH}$, $R_1 = R_2 = 0.1 \Omega$, $C = 5 \mu\text{F}$. The current simulation curve with repetitive control is shown in Fig. 10.

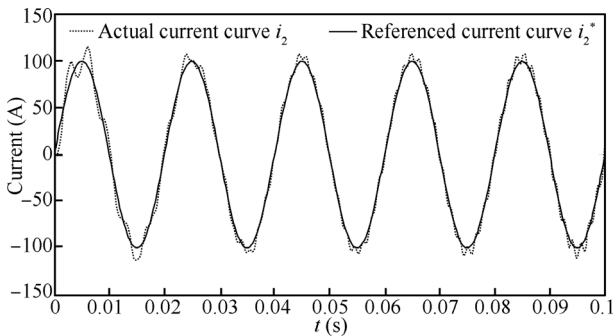


Fig. 10 The current curve with repetitive control and system parameters changed

The error curve is as shown in Fig. 11, after the system parameters are changed:

When the system parameters are changed, simulation curve is shown in Fig. 12, adopting robust iterative learning control.

The error curve is as shown in Fig. 13, after system parameters are changed.

When the system parameters are changed, the robust iterative learning control prove to be better than repetitive control in robustness, the former can ensure the accuracy of the output waveform as shown in Figs. 10–13.

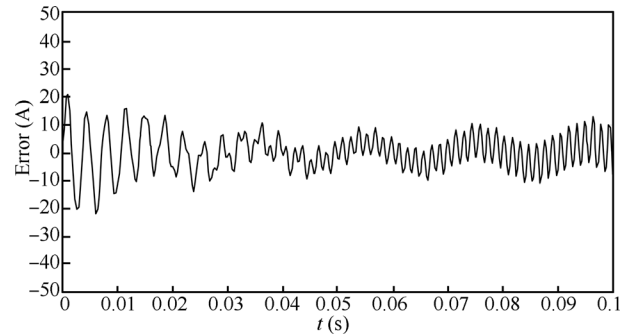


Fig. 11 The error current curve with repetitive control and system parameters changed

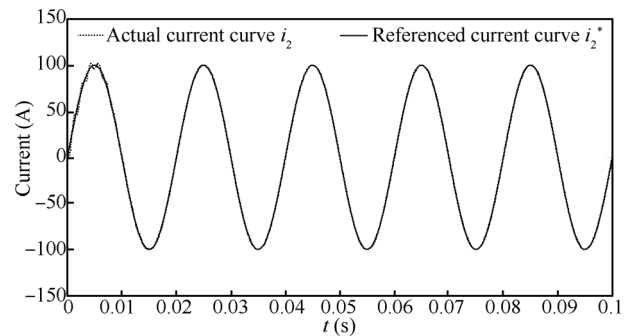


Fig. 12 The current curve with robust iterative learning control and system parameters changed

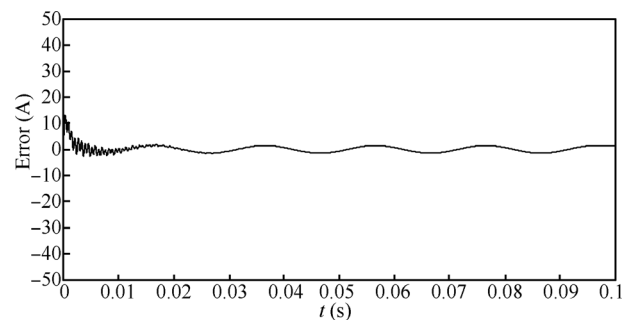


Fig. 13 The current error curve with system parameters changed

In the following, we will test the current sharing effect of two grid-connected inverters with robust iterative learning control. Firstly, let the inverter 1 run, the inverter 2 would merge into power grid after 0.2 s, and initial phase difference

of two inverters is 2.1° as shown in [18]. Set $\Delta\omega_{\max} = 0.04$, $P_{e1} = 1000$ W, $P_{e2} = 500$ W, $\Delta E_{\max} = 0.03$, $Q_{e1} = 600$ W, $Q_{e2} = 1000$ W. According to (4) and (5), set the parameters of power droop characteristic: $m_1 = 4.0 \times 10^{-5}$, $n_1 = 5 \times 10^{-5}$, $m_2 = 8 \times 10^{-5}$, $n_2 = 3.0 \times 10^{-5}$, the current curve of inverters 1 and 2 are shown in Fig. 14.

From Fig. 14, it is shown that when inverter 2 is connected with the utility grid, the output current of inverters 1 and 2 are almost the same at 0.05 s. The precision of error current is less than 10^{-4} , and synchronous operation is achieved accurately between the two inverters.

The current curve of inverters 1 and 2 after the system parameters are changed is shown in Fig. 15.

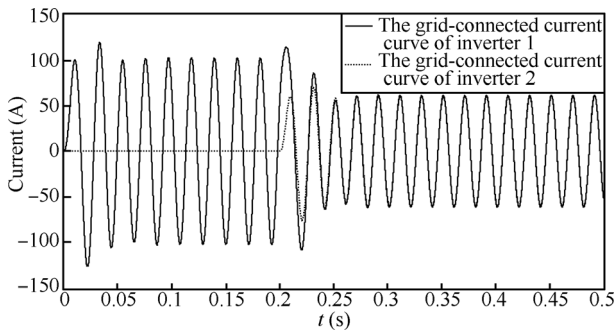


Fig. 14 The current curve of inverters 1 and 2

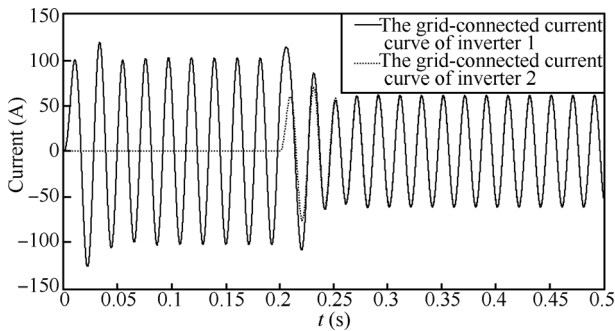


Fig. 15 The current curve of two inverters with system parameters changed

When the system parameters are changed, let the inverter 2 merge into the utility grid at 0.2 s. Through 0.05 s iterative learning, synchronous operation can still be achieved accurately. It shows that the system have strong robustness.

7 Conclusions

In this paper, adopting no interconnection line control mode based on power droop characteristic, the synchronous operation of single-phase LCL grid-connected inverter in micro-grid is realized among the inverters. The structure is simple, and the current sharing effect is marked. A kind of robust iterative learning controller is designed by the robust performance index, which is suitable to repeated tracking control and periodic disturbance rejection, and has the ability to overcome uncertainty of system parame-

ters. It shows that the robust iterative learning control can solve the distortion of the output signal effectively, and improve the tracking performance for waveform. The accurate synchronous operation is achieved among the inverters as shown through the simulation.

References

- [1] N. Hatzigiorgiou, H. Asano, R. Iravani, C. Marnay. Microgrids. *IEEE Power and Energy Magazine*, vol. 5, no. 4, pp. 78–94, 2007.
- [2] H. H. Yang, G. W. Yu, Z. F. Fan, H. M. Zhu, D. Q. Bi. The development and application of micro-grid system controller. *Power System Protection and Control*, vol. 39, no. 19, pp. 126–129, 140, 2011. (in Chinese)
- [3] H. G. Jeong, K. B. Lee, S. Choi, W. Choi. Performance improvement of LCL-filter-based grid-connected inverters using PQR power transformation. *IEEE Transactions on Power Electronics*, vol. 25, no. 5, pp. 1320–1330, 2010.
- [4] T. Yu, S. Choi, H. Kim. Indirect current control algorithm for utility interactive inverters for seamless transfer. In *Proceedings of the 37th IEEE Power Electronics Specialists Conference*, IEEE, Jeju, Korea, pp. 1–6, 2006.
- [5] X. Q. Guo, W. Y. Wu, H. R. Gu, L. Q. Wang, Q. L. Zhao. Modelling and stability analysis of direct output current control for LCL interfaced grid-connected inverters. *Transactions of China Electrotechnical Society*, vol. 25, no. 3, pp. 102–109, 2010. (in Chinese)
- [6] Z. Q. Wu, J. P. Xie. Design of adaptive robust guaranteed cost controller for wind power generator. *International Journal of Automation and Computing*, vol. 10, no. 2, pp. 111–117, 2013.
- [7] D. Li, J. M. Li. Adaptive iterative learning control for nonlinearly parameterized systems with unknown time-varying delay and unknown control direction. *International Journal of Automation and Computing*, vol. 9, no. 6, pp. 578–586, 2012.
- [8] A. Garcia-Cerrada, O. Pinzon-Ardila, V. Feliu-Batlle, P. Roncero-Sanchez, P. Garcia-Gonzalez. Application of a repetitive controller for a three-phase active power filter. *IEEE Transactions on Power Electronics*, vol. 22, no. 1, pp. 237–246, 2007.
- [9] J. Dannehl, C. Wessels, F. W. Fuchs. Limitations of voltage-oriented PI current control of grid-connected PWM rectifiers with LCL filters. *IEEE Transactions on Industrial Electronics*, vol. 56, no. 2, pp. 380–388, 2009.
- [10] S. J. Yu, X. D. Qi, J. H. Wu. *Iterative Learning Control Theory and Application*, Beijing: Machinery Industry Press, 2005. (in Chinese)
- [11] T. Liu, Y. Q. Wang. A synthetic approach for robust constrained iterative learning control of piecewise affine batch processes. *Automatica*, vol. 48, no. 11, pp. 2762–2775, 2012.

- [12] C. Olalla, I. Queinnec, R. Leyva, A. El Aroudi. Robust optimal control of bilinear DC-DC converters. *Control Engineering Practice*, vol. 19, no. 7, pp. 688–699, 2011.
- [13] H. Moradi, F. Bakhtiari-Nejad, M. Saffar-Avval. Multivariable robust control of an air-handling unit: A comparison between pole-placement and H_∞ controllers. *Energy Conversion and Management*, vol. 55, pp. 136–148, 2012.
- [14] S Y. Yang, A. Luo, X P. Fan. Adaptive robust iterative learning control for uncertain robotic systems. *Control Theory and Applications*, vol. 20, no. 5, pp. 707–712, 2003. (in Chinese)
- [15] M. Wu. *The Modern Robust Control*, Changsha: Central South University Press, 2006. (in Chinese)
- [16] K. J. Aström, T. Hägglund. Revisiting the Ziegler-Nichols step response method for PID control. *Journal of Process Control*, vol. 14, no. 6, pp. 635–650, 2004.
- [17] N. M. Seal. Repetitive control. *Encyclopedia of the Sciences of Learning*, New York: Springer, 2012.
- [18] H. R. Karshenas, H. Sashimi. Basic criteria in designing LCL filters for grid connected converters. In *Proceedings of 2006 IEEE International Symposium on Industrial Electronics*, IEEE, Montreal, Canada, vol. 3, pp. 1996–2000, 2006.



Zhong-Qiang Wu received his B.Sc. and M.Sc. degrees in automatic control from Northeast Heavy Machinery Institute, China in 1989 and 1992, respectively, and his Ph.D. degree in control theory and control engineering from China University of Mining and Technology, China in 2003. He is a professor at the College of Electrical Engineering, Yanshan University, China.

His research interests include intelligent control of wind power system.

E-mail: mewzq@163.com (Corresponding author)



Chun-Hua Xu received his B. Eng. degree in automation from Luoyang Institute of Science and Technology, China in 2011. He is currently a master student in control theory and control engineering at College of Electrical Engineering, Yanshan University, China.

His research interests include intelligent control of wind power system.

E-mail: muzhiqinghan@163.com



Yang Yang received her B. Eng. degree in automation from Baoji University of Art and Technology, China in 2011. She is currently a master student in control theory and control engineering at College of Electrical Engineering, Yanshan University, China.

Her research interests include intelligent control of wind power system.

E-mail: yangyangyang6380@163.com